Ionization equilibrium in an excited semiconductor: Mott transition versus Bose-Einstein condensation

D. Semkat, F. Richter, D. Kremp, G. Manzke, W.-D. Kraeft, and K. Henneberger
Institut für Physik, Universität Rostock, 18051 Rostock, Germany
(Received 15 June 2009; revised manuscript received 4 September 2009; published 2 October 2009)

The ionization equilibrium of an electron-hole plasma in a highly excited semiconductor is investigated. Special attention is directed to the influence of many-particle effects such as screening and lowering of the ionization energy causing, in particular, the Mott effect (density ionization). This effect limits the region of existence of excitons and, therefore, of a possible Bose-Einstein condensate at low temperatures. Results for the chemical potential and the degree of ionization are presented for zinc selenide (ZnSe). A possible window for the occurrence of a Bose-Einstein condensate of excitons is shown, taking into account the Mott effect.

DOI: 10.1103/PhysRevB.80.155201 PACS number(s): 71.35.Ee, 71.35.Lk, 03.75.Hh, 03.75.Kk

I. INTRODUCTION

Dense electron-hole plasmas (EHPs) in excited semiconductors have attracted unwaning attention for decades both by experiment and theory. The understanding of the equilibrium properties of such a plasma, expressed by its phase diagram, is of fundamental importance for any investigation in this field. The aim of this paper is, therefore, to discuss certain aspects of the phase diagram of an EHP: the ionization equilibrium and, closely connected with the latter, the Mott transition.

Electrons and holes are Fermi particles with the effective masses m_e and m_h (parabolic valence and conduction bands). Due to the attractive Coulomb interaction between them, bound electron-hole pairs, the excitons, and the formation of an ionization equilibrium $e+h \rightleftarrows X$ are observed.

The behavior of an EHP in an excited semiconductor is, in principle, well understood.[1,2] A special feature is the weakening of the coupling with increasing density caused by many-particle effects such as screening of the Coulomb interaction and, therefore, a breakup of the excitons usually referred to as Mott effect (density ionization).[3–6]

The Mott effect is, in principle, understood as caused by lowering of the band edge, while the exciton energy only weakly changes with increasing density. This behavior is caused by an interplay of several many-particle effects. There are various approaches which can be found in the literature to describe the Mott effect, e.g., simple limiting cases known from quantum statistics such as Debye shift or Coulomb-hole shift for the band edge as well as statistically founded or empirical formulas for the Mott density in semiconductors (see, e.g., Refs. 7–9). Such formulas, however, are far away from the capabilities of modern many-particle theory and usually do not give more than a rough estimate. On the other hand, previous investigations of the ionization equilibrium[10] neglected degeneracy effects, e.g., by using the Saha equation. For this, a central aim of this work is to present a consistent quantum statistical theory of the ionization equilibrium and provide reliable data for the temperature dependence of the Mott density. A first step into that direction has been done in Ref. 11, where a general mass-action law (MAL) has been derived and applied to the ionization equilibrium in cuprous oxide (Cu_2O). A self-contained presentation of the theory together with a consistent treatment of the many-particle effects will be given in the present work.

A qualitative overview of the different states of the EHP which could guide in particular experimentalists in the choice of parameters for experiments can be given in the density-temperature (n-T) plane. Because of the Mott effect, which occurs roughly at $r_{sc} \simeq a_X$ (r_{sc} denotes the screening length, a_X the excitonic Bohr radius), the n-T plane is divided into an area where bound states are possible ($r_{sc} > a_X$) and an area without bound states ($r_{sc} < a_X$), i.e., a high-density electron-hole liquid. This subdivision, however, can only give a qualitative picture.

The behavior in the excitonic area is essentially governed by the formation of an ionization equilibrium, with a strong dominance of excitons at lower temperatures. Since the excitons behave approximately like composite Bose particles, Bose-Einstein condensation (BEC) in the region $n\Lambda_X^3 \geq 2.61$ [Λ_X is the thermal de Broglie wavelength, $\Lambda_X^2 = 2\pi\hbar^2/(Mk_BT)$, $M=m_e+m_h$] may be expected if the chemical potential reaches the exciton $1s$ ground-state energy.[12–14] At higher densities, the region of BEC of excitons is, of course, limited by the Mott transition. However, we underline that the vanishing of the excitons does not imply a disappearance of the condensed phase. As proposed, e.g., by Keldysh and Kopaev,[15] in the high-density highly degenerate electron-hole liquid, the formation of weakly bound cooperative Cooper pairs of electrons and holes and their Bose condensation to a BCS state may be expected, known as excitonic insulator. Details of BEC of excitons and electron-hole pairs, however, are not in the main focus of the present work. For an overview and recent investigations see, e.g., Refs. 16–19.

The ionization equilibrium is a topic which is extensively discussed in plasma physics, too.[2,20,21]

This paper is organized as follows. In Sec. II we derive briefly the basic quantum statistical theory of thermodynamics of the EHP. In Sec. III we introduce the chemical picture by redefining the bound states and discuss the resulting mass-action law. Since the latter needs the solution of the two-particle bound and scattering problem as an input, we discuss, in Sec. IV, the two-particle spectrum on the basis of the semiconductor Bloch equations. Finally, in Sec. V we present results of the solution of the general mass-action law valid for arbitrary degeneracy.

II. GENERAL THEORY

There are several possibilities for the quantum statistical approach to the equilibrium properties of the EHP, outlined, e.g., in Refs. 1, 21, and 22. For a better understanding, we will give a short review of the approach used here to describe the ionization equilibrium. A useful starting point is the general quantum statistical relation

$$n_a(\{\mu_c\},T) = g_a \int \frac{d\mathbf{k}}{(2\pi)^3} \int \frac{d\omega}{2\pi} A_a(\mathbf{k},\omega) f_a(\omega), \tag{1}$$

expressing the carrier density n_a of the species a as a function of the chemical potentials $\{\mu_c\}$ and the temperature T. $f_a(\omega)$ is a Fermi-like distribution, and g_a denotes the band multiplicity (including spin degeneracy) of species a. The spectral function $A_a(\mathbf{k},\omega) = -2\ \mathrm{Im}\ g_a^r(\mathbf{k},\omega)$ is related to the imaginary part of the retarded Green's function of carriers $g_a^r(\mathbf{k},\omega)$ and is explicitly given by[21]

$$A_a(\mathbf{k},\omega) = \frac{\hbar\Gamma_a(\mathbf{k},\omega)}{\left[\hbar\omega - \frac{\hbar^2k^2}{2m_a} - \mathrm{Re}\ \Sigma_a^r(\mathbf{k},\omega)\right]^2 + \left[\frac{1}{2}\Gamma_a(\mathbf{k},\omega)\right]^2}, \tag{2}$$

with the single-particle damping Γ_a defined by the self-energies $\Sigma_a^{\gtrless}$,

$$\Gamma_a(\mathbf{k},\omega) = -2\ \mathrm{Im}\ \Sigma_a^r(\mathbf{k},\omega) = i[\Sigma_a^>(\mathbf{k},\omega) - \Sigma_a^<(\mathbf{k},\omega)]. \tag{3}$$

The spectral function accounts for many-particle effects compactly in the retarded self-energy $\Sigma_a^r(\mathbf{k},\omega)$. With an appropriate approximation for the self-energy, the inversion of Eq. (1) gives $\mu_a = \mu_a(n_a,T)$ and, therefore, any thermodynamic property of the EHP in the grand canonical description.

In the case of small damping, i.e., $\Gamma_a \ll \mathrm{Re}\ \Sigma_a^r$, we can expand the spectral function into a series with respect to Γ_a. The first-order approximation reads[23,24]

$$A_a(\mathbf{k},\omega) = 2\pi\hbar\,\delta[\hbar\omega - E_a(\mathbf{k})] \times \left[1 + \frac{1}{\hbar}\frac{\partial}{\partial\omega}\mathcal{P}\int \frac{d\bar{\omega}}{2\pi}\ \frac{\Gamma_a(\mathbf{k},\bar{\omega})}{\omega - \bar{\omega}}\bigg|_{\hbar\omega = E_a(\mathbf{k})}\right] - \Gamma_a(\mathbf{k},\omega)\frac{\partial}{\partial\omega}\frac{\mathcal{P}}{\hbar\omega - E_a(\mathbf{k})}, \tag{4}$$

where $\mathcal{P}$ denotes the Cauchy principal value. The quasiparticle energy $E_a(\mathbf{k})$ is the solution of the dispersion relation

$$E_a(\mathbf{k}) = \frac{\hbar^2k^2}{2m_a} + \mathrm{Re}\ \Sigma_a^r(\mathbf{k},\omega)\big|_{\hbar\omega = E_a(\mathbf{k})}. \tag{5}$$

The approximation (4) is referred to as *extended quasiparticle approximation*.[24] Its physical interpretation is clear: The first (pole) contribution describes the free quasiparticles, including renormalization, the second (off-pole) term represents the interaction between the quasiparticles. Using the expansion (4), the carrier density is given by[23,24]

$$\begin{aligned} n_a(\{\mu_c\},T) &= g_a \int \frac{d\mathbf{k}}{(2\pi)^3} f_a(E_a(\mathbf{k})) - g_a \int \frac{d\mathbf{k}}{(2\pi)^3} \int \frac{d\omega}{2\pi} \\ &\times \left\{ \Gamma_a(\mathbf{k},\omega)[f_a(\omega) - f_a(E_a(\mathbf{k}))] \frac{\partial}{\partial\omega}\frac{\mathcal{P}}{\hbar\omega - E_a(\mathbf{k})} \right\} \\ &= n_a^0 + n_a^{\mathrm{corr}}. \end{aligned} \tag{6}$$

The total density n_a is, therefore, subdivided into a contribution of the free quasiparticles n_a^0 and the correlated ones n_a^{corr} (second virial coefficient for quasiparticles).

We proceed with the following steps:

(i) Obviously, the function Γ_a is a key quantity of the theoretical approach. For its determination, there exist well-known standard approximation schemes.[21,22] In order to address the problems of screening and forming of bound states we consider the self-energy and, therefore, the damping Γ_a in screened ladder approximation[1,2]

$$\Gamma_a(\mathbf{k}_1,\omega) = -2\sum_b \int \frac{d\mathbf{k}_2}{(2\pi)^3} \mathrm{Im}\langle \mathbf{k}_1\mathbf{k}_2|T_{ab}^r(\omega + E_b(\mathbf{k}_2))|\mathbf{k}_1\mathbf{k}_2\rangle \times [f_b(E_b(\mathbf{k}_2)) \mp n_{ab}^B(\omega + E_b(\mathbf{k}_2))]. \tag{7}$$

The retarded off-shell T matrix obeys a Bethe-Salpeter (or Lippmann-Schwinger) equation, $T_{ab}^r = V_{ab}^s + i\hbar V_{ab}^s \mathcal{G}_{ab}^r T_{ab}^r$, where V_{ab}^s is the screened Coulomb potential, and $\mathcal{G}_{ab}^r$ is the free two-particle retarded Green's function given by the single-particle correlation functions $g_a^{\gtrless}$ via

$$\mathcal{G}_{ab}^r(\omega) = \int \frac{d\bar{\omega}}{2\pi} \int \frac{d\bar{\bar{\omega}}}{2\pi} \frac{g_a^>(\bar{\omega}) g_b^>(\bar{\bar{\omega}}) - g_a^<(\bar{\omega}) g_b^<(\bar{\bar{\omega}})}{\omega - \bar{\omega} - \bar{\bar{\omega}} + i\epsilon}. \tag{8}$$

(ii) To be consistent with the Γ_a expansion of the spectral function, we expand the distribution function according to[25]

$$f_a(\epsilon_a + \mathrm{Re}\ \Sigma_a'') \approx f_a(\epsilon_a) + \mathrm{Re}\ \Sigma_a'' \frac{df}{d\epsilon_a}, \tag{9}$$

where

$$\epsilon_a(\mathbf{k}) = \frac{\hbar^2k^2}{2m_a} + \mathrm{Re}\ \Sigma_a^{\mathrm{RPA}}(\mathbf{k},\omega)\big|_{\hbar\omega = \epsilon_a(\mathbf{k})} \tag{10}$$

is the quasiparticle energy in *random phase approximation* (RPA) including the Hartree-Fock (HF) self-energy Σ_a^{HF}, and Σ_a'' means higher-order ladder terms convergent also for vanishing screening.

(iii) Inserting Eqs. (7) and (9) into Eq. (6), we get for the density

$$n_a(\{\mu_c\},T) = g_a \int \frac{d\mathbf{k}}{(2\pi)^3} f_a(\epsilon_a(\mathbf{k})) + g_a \sum_b \int_{-\infty}^{\infty} \frac{d\omega}{2\pi} n_{ab}^B(\omega)\,\mathrm{Im}\ F(\omega) \tag{11}$$

with

$$F(\omega) = \mathrm{Tr}_{12}\left[\frac{d}{d\omega}\mathcal{G}_{ab}^r(\omega) T_{ab}^r(\omega)\right].$$

The main concern of our approach is to describe the influence of bound states on the properties of an EHP. Bound and scattering state contributions arise from the off-pole terms in Eq. (6) determined in screened ladder approximation by the off-shell T matrix, see Eq. (7). The bound states appear in the off-shell T matrix as poles at the real frequency axis. From the bilinear expansion of the T matrix, we obtain for the bound state part[1,21,26]

$$F^{\text{bound}}(\omega) = \sum_{n,l} \pi(2l+1)\,\delta(\hbar\omega - E_{nl}),$$

with E_{nl} being the bound state energy of the level given by the set of quantum numbers $\{n,l\}$. Using this relation, the bound and scattering state parts for the electron density may be separated,

$$n_e(\mu_e,\mu_h,T) = g_e \int \frac{d\mathbf{k}}{(2\pi)^3} f_e(\epsilon_e(\mathbf{k})) + g_e g_h \sum_{nl} (2l+1) \int \frac{d\mathbf{K}}{(2\pi)^3} \times \frac{1}{\exp\left[\beta\left(\frac{\hbar^2K^2}{2M} + E_{nl} - \mu_e - \mu_h\right)\right] - 1} + g_e \int_\Delta^\infty \frac{d\omega}{2\pi} n_{eh}^B(\omega)\,\text{Im}\,F(\omega) \tag{12}$$

with Δ representing the lowering of the band (continuum) edge and $\beta=(k_BT)^{-1}$. The first term in Eq. (12) is the density of the free quasiparticles. The second term is the contribution of bound states,[1,2,25] and the third one that of scattering states.

III. CHEMICAL PICTURE

Up to now we considered the EHP in grand canonical description as a two-component system with electrons and holes in scattering and bound states. This description is usually referred to as the physical picture. Then, Eq. (12) provides appropriate thermodynamics of the plasma. In contrast, the density expansion of the chemical potential following by approximate inversion of Eq. (12) leads to inconsistencies at low temperatures due to exponential divergences of the bound state part.[2,21]

In the following we briefly recall an alternative view on the bound states.[2] Looking at the corresponding distribution function

$$n_{eh}^B\left(\frac{\hbar^2K^2}{2M} + E_{nl}\right) = \frac{1}{z_e^{-1}z_h^{-1}\exp\left[\beta\left(E_{nl} + \frac{\hbar^2K^2}{2M}\right)\right] - 1} \tag{13}$$

with the fugacities $z_a=e^{\beta\mu_a}$, it is, obviously, convenient to consider *bound states as a new particle species (excitons)*, which are characterized by the fugacity z_X,

$$z_X = z_e z_h e^{-\beta E_{nl}} = e^{\beta\mu_X} \tag{14}$$

and by the ideal distribution function

$$n_X^B\left(\frac{\hbar^2K^2}{2M}\right) = \frac{1}{z_X^{-1}\exp\left[\beta\frac{\hbar^2K^2}{2M}\right] - 1}. \tag{15}$$

With the latter step we have made a fundamental change from the physical picture where the basic constituents are only electrons and holes, being in scattering or bound states, to a chemical picture where we have electrons, holes, and excitons as basic constituents of the system.

We should emphasize here, however, the limitations of this picture or, more precisely, of the underlying extended quasiparticle approximation for the spectral function $A_a(\mathbf{k},\omega)$, Eq. (4): While $A_a(\mathbf{k},\omega)$ exhibits, at lower densities, distinct bound state peaks and the pair continuum, the peaks broaden for higher densities due to the damping. Thus, a well-defined distinction between bound and scattering states becomes problematic around the Mott density.[5,6,27] A quantitative demonstration of the effect for zinc oxide (ZnO) has been given by Klingshirn, see Fig. 24b in Ref. 28. However, in ZnSe the excitonic linewidth is much smaller,[38] as will be discussed in Sec. IV.

The electron density in the chemical picture consists of "free" (quasiparticle n_e^{QP} and scattering n_e^{scatt}) and the bound (exciton) n_X contributions, cf. Eq. (12),

$$\begin{aligned} n_e(\mu_e,\mu_h,\mu_X,T) &= g_e \int \frac{d\mathbf{k}}{(2\pi)^3} f_e(\epsilon_e(\mathbf{k})) \\ &\quad + g_e \int_\Delta^\infty \frac{d\omega}{2\pi} n_{eh}^B(\omega)\,\text{Im}\,F(\omega) \\ &\quad + g_e g_h \sum_{nl} (2l+1) \int \frac{d\mathbf{K}}{(2\pi)^3} n_X^B\left(\frac{\hbar^2K^2}{2M}\right) \\ &= n_e^{\text{QP}} + n_e^{\text{scatt}} + n_X. \end{aligned} \tag{16}$$

The excitons consisting of two bound Fermi particles are described approximately as bosons [cf. Eqs. (13) and (15)]. The singularities of the bound state contribution $E_{nl}+\hbar^2K^2/(2M)=\mu_e+\mu_h$ are well known to be connected to the Bose condensation of the excitons.

In the chemical picture, the EHP is characterized by the densities of free electrons $n_e^*=n_e^{\text{QP}}+n_e^{\text{scatt}}$, free holes n_h^* (with $n_h^*=n_e^*$), and the density of excitons n_X (total electron density $n_e=n_e^*+n_X$). We have a partially ionized plasma in the ionization equilibrium

$$e + h \rightleftarrows X, \tag{17}$$

which is controlled by the definition of the fugacities of the new particles (14). The latter relation determines the composition of the system described by the degree of ionization

$$\alpha = \frac{n_e^*}{n_e} \tag{18}$$

and plays the role of a MAL. It is equivalent to the well-known thermodynamic condition for the chemical (ionization) equilibrium

$$\mu_X = \mu_e + \mu_h - E_{nl}. \tag{19}$$

In the grand canonical description, the condition (19) is just a consequence of the definition of excitons, Eqs. (14) and (15). The chemical potential of the excitons μ_X is given by the inversion of

$$n_X(\mu_X,T) = g_e g_h \int \frac{d\mathbf{K}}{(2\pi)^3} \frac{1}{\exp\left[\beta\left(\frac{\hbar^2 K^2}{2M} - \mu_X\right)\right] - 1}. \tag{20}$$

We should again stress the fact that the degree of ionization is, due to the damping of the two-particle states, not really a well-defined quantity around the Mott density. It gives, however, a good qualitative measure for the state of the EHP.

From the previous consideration, in principle, the chemical potential of free carriers (neglecting scattering states) is known, too. It is defined by

$$n_a^*(\mu_a,T) = g_a \int \frac{d\mathbf{k}}{(2\pi)^3} \frac{1}{e^{\beta[\epsilon_a(\mathbf{k})-\mu_a]} + 1}. \tag{21}$$

An analytical determination of the chemical potential from Eq. (21) is possible at most in limiting cases (nondegenerate or highly degenerate, respectively). In the general case, knowing the RPA quasiparticle energy $\epsilon_a(\mathbf{k})$, μ_a can be obtained by numerical inversion of Eq. (21). The determination of $\epsilon_a(\mathbf{k})$ according to Eq. (10) is, however, a numerically expensive task. As an alternative to the *complete inversion* of Eq. (21), one can split the chemical potential according to[2,25]

$$\mu_a = \mu_a^{\mathrm{id}} + \Delta\mu_a. \tag{22}$$

Here, μ_a^{id} is the ideal contribution and $\Delta\mu_a$ is the correlation part. The inversion of Eq. (21) with respect to the first order in $\Delta\mu_a$ is usually referred to as *incomplete inversion*.[29] Then the ideal contribution, for arbitrary degeneracy, follows in well-known manner from

$$n_a^*(\mu_a^{\mathrm{id}},T) = g_a \int \frac{d\mathbf{k}}{(2\pi)^3} \frac{1}{\exp\left[\beta\left(\frac{\hbar^2 k^2}{2m_a} - \mu_a^{\mathrm{id}}\right)\right] + 1}. \tag{23}$$

Numerical calculations for the correlation part $\Delta\mu_a$ have been performed, e.g., for a hydrogen plasma in Ref. 29 and for the EHP in Ref. 30. From the numerical results and the limiting cases, Padé formulas have been constructed in Refs. 30 and 31. A formula very similar to that in Ref. 30 has been proposed in Ref. 1.

With the subdivision (22) for the chemical potential of the species a introduced above, and $\Delta\mu_{eh}=\Delta\mu_e+\Delta\mu_h$, a generalized MAL follows from Eq. (14),

$$z_X = e^{\beta\mu_e^{\mathrm{id}}} e^{\beta\mu_h^{\mathrm{id}}} e^{-\beta(E_{nl}-\Delta\mu_{eh})}, \tag{24}$$

which determines the plasma composition implicitly.

The procedure is simpler for a nondegenerate EHP. Then it holds

$$z_a = \frac{n_a \Lambda_a^3}{g_a} e^{\beta\Delta\mu_a}, \quad z_X = \frac{n_X \Lambda_X^3}{g_e g_h} \tag{25}$$

with $\Lambda_a^2 = 2\pi\hbar^2/(m_a k_B T)$, and we immediately arrive at the Saha equation for nonideal plasmas,[2,10]

$$\frac{1-\alpha}{\alpha^2} = n_e \Lambda_{eh} e^{-\beta(E_{nl}-\Delta\mu_{eh})} \tag{26}$$

with $\Lambda_{eh}^2 = 2\pi\hbar^2/(m_{eh} k_B T)$, $m_{eh}^{-1} = m_e^{-1} + m_h^{-1}$. For arbitrary degeneracy, the degree of ionization α has to be determined by Eq. (19) and (24) instead of the Saha Eq. (26). In terms of α and n_e, Eq. (19) gets the form

$$\mu_X[(1-\alpha)n_e,T] = \mu_e[\alpha n_e,T] + \mu_h[\alpha n_e,T] - E_{nl}. \tag{27}$$

Equation (27) represents a form of the MAL defined by Eq. (14), which allows for the determination of the degree of ionization α as a function of density and temperature and, therefore, can be regarded as a generalized Saha equation. The degree of ionization is given implicitly by Eq. (27) and has to be obtained numerically.[11]

IV. ELECTRON-HOLE PAIR SPECTRUM

The influence of many-body effects on the composition of the partially ionized EHP according to Eqs. (27) together with Eqs. (21) and (20) is contained in two quantities, namely, (i) the quasiparticle energies $\epsilon_a(\mathbf{k})$ and (ii) the two-particle bound state (exciton) energy E_{nl}. It is well known from both optical experiments[32] and from the theoretical point of view[3] that the exciton energy only weakly changes with increasing excitation, while the ionization is mainly generated by the lowering of the band edge, described in our approach by the quasiparticle energies of carriers. According to Ref. 3, this behavior can be described by an effective wave equation considering the influence of screening both by self-energies and by a renormalization of the Coulomb interaction.

Experimentally the influence of many-body effects in an excited semiconductor can be determined by measuring the optical spectrum detected with a weak probe pulse. A corresponding theoretical description is given by the semiconductor Bloch equations (SBEs).[33] If one considers the carriers to be in quasiequilibrium, the carrier distributions are Fermi functions with given chemical potential and temperature, which are not affected by the weak probe pulse, and only the kinetic equation for the polarization has to be solved. In this case, the equation for the polarization $p(\mathbf{k},\omega)$, generated by the probe pulse $E(\omega)$ and coupled via the dipole matrix element d to the semiconductor, can be written in excitonic units as[34–38]

$$\{\omega - \mathbf{k}^2 - \Delta^{\mathrm{HF}}(\mathbf{k}) - \Sigma^r(\mathbf{k},\omega)\}p(\mathbf{k},\omega) + \int \frac{d\mathbf{q}}{(2\pi)^3}\{N(\mathbf{k})V_{eh}(\mathbf{k}-\mathbf{q}) + \Theta(\mathbf{k},\mathbf{q},\omega)\}p(\mathbf{q},\omega) = N(\mathbf{k})dE(\omega). \tag{28}$$

Many-body effects are contained (i) as HF renormalized carrier energies $\Delta^{\mathrm{HF}}(\mathbf{k})$ and Pauli blocking $N(\mathbf{k})=1-f_e(\mathbf{k})$

$-f_h(\mathbf{k})$, and (ii) as screening effects in the renormalized interaction matrix $\Theta(\mathbf{k},\mathbf{q},\omega)$,

$$\Theta(\mathbf{k},\mathbf{q},\omega) = \Delta V^{\mathrm{eff}}(\mathbf{k},\mathbf{q},\omega) - i\Gamma(\mathbf{k},\mathbf{q},\omega)$$
$$= \sum_{a\neq b}\int \frac{d\bar{\omega}}{2\pi} \times \frac{[1-f_a(\mathbf{k})]V_{ab}^{>}(\mathbf{k}-\mathbf{q},\bar{\omega}) + f_a(\mathbf{k})V_{ab}^{<}(\mathbf{k}-\mathbf{q},\bar{\omega})}{\hbar\omega - \epsilon_a(\mathbf{k}) - \epsilon_b(\mathbf{q}) - \hbar\bar{\omega} + i[\Gamma_a(\mathbf{k}) + \Gamma_b(\mathbf{q})]/2}, \tag{29}$$

whose real and imaginary parts, $\Delta V^{\mathrm{eff}}(\mathbf{k},\mathbf{q},\omega)$ and $\Gamma(\mathbf{k},\mathbf{q},\omega)$, are the effective interaction and the so-called off-diagonal dephasing, respectively, and in the interband self-energy $\Sigma^r(\mathbf{k},\omega)$,

$$\Sigma^r(\mathbf{k},\omega) = \Delta e^{sc}(\mathbf{k},\omega) - i\Gamma(\mathbf{k},\omega) = \int \frac{d\mathbf{q}}{(2\pi)^3}\Theta(\mathbf{q},\mathbf{k},\omega)$$
$$= \Sigma_e^r(\mathbf{k},\omega-\epsilon_h) + \Sigma_h^r(\mathbf{k},\omega-\epsilon_e), \tag{30}$$

with its real and imaginary parts $\Delta e^{sc}(\mathbf{k},\omega)$ and $\Gamma(\mathbf{k},\omega)$ being the renormalized interband self-energy and the diagonal dephasing, respectively.

It is important to notice that the various many-body quantities widely compensate each other pairwise in the case of bound states. This concerns on one hand the HF energies and the Pauli blocking, and the renormalized interband self-energy $\Delta e^{sc}(\mathbf{k},\omega)$ and the effective interaction $\Delta V^{\mathrm{eff}}(\mathbf{k},\mathbf{q},\omega)$ on the other hand as well as the so-called diagonal and off-diagonal dephasing $\Gamma(\mathbf{k},\omega)$, $\Gamma(\mathbf{k},\mathbf{q},\omega)$, respectively. Moreover, there is an exact relation of the (two-particle) interband self-energy Σ^r for an energy $\hbar\omega$ to the (single-particle) carrier self-energies Σ_a^r at shifted energies $\hbar\omega-\varepsilon_b$ given in Eq. (30). The appearance of this energy shift becomes physically clear if one looks at the energies in the denominator of the effective interaction matrix $\Theta(\mathbf{k},\mathbf{q},\omega)$. It becomes resonant if the incident photon with the energy $\hbar\omega$ generates an interband transition, described by the renormalized quasiparticle energies $\varepsilon_a(\mathbf{k})+\varepsilon_b(\mathbf{q})$, accompanied by absorption or emission of a plasmon with the energy $\hbar\bar{\omega}$. The quasiparticle energies $\varepsilon_a(\mathbf{k})$ and the quasiparticle damping $\Gamma(\mathbf{k},\omega)$ here are determined from Eqs. (10) and (3) using the RPA self-energy

$$\Sigma_a^{\gtrless}(\mathbf{k},\omega) = \int \frac{d\mathbf{q}}{(2\pi)^3}\int \frac{d\omega'}{2\pi} g_a^{\gtrless}(\mathbf{k}-\mathbf{q},\omega-\omega')V_{aa}^{\gtrless}(\mathbf{q},\omega'). \tag{31}$$

The correlation functions of the screened potential $V_{ab}^{\gtrless}(\mathbf{q},\omega)$ appearing in the Eqs. (29)–(31) are related to the inverse retarded dielectric function $\varepsilon^{r^{-1}}(\mathbf{q},\omega)$ via

$$V_{ab}^{<}(\mathbf{q},\omega) = 2iV_{ab}(\mathbf{q})\mathrm{Im}\ \varepsilon^{r^{-1}}(\mathbf{q},\omega)n^B(\omega),$$
$$V_{ab}^{>}(\mathbf{q},\omega) = 2iV_{ab}(\mathbf{q})\mathrm{Im}\ \varepsilon^{r^{-1}}(\mathbf{q},\omega)[1+n^B(\omega)]. \tag{32}$$

The function $n^B(\omega)$ represents the Bose distribution of the elementary excitations in the plasma (plasmons), and, in our calculations, we use the Lindhard dielectric function. Contributions of bound electron-hole pairs to the dielectric screening function in the sense of atomic (excitonic) polarizabilities[39] are small as compared to that of the free carriers and are neglected. This is justified if the description of the Mott transition is addressed; however, excitonic contributions to screening should be incorporated if the properties of the pure excitonic gas phase are investigated.

For weak probe pulses the macroscopic polarization $P(\omega)$ depends linearly on the electric field

$$P(\omega) = \int \frac{d\mathbf{k}}{(2\pi)^3} p(\mathbf{k},\omega) = \chi(\omega)E(\omega), \tag{33}$$

where the susceptibility $\chi(\omega)$ characterizes the dielectric properties of the semiconductor. The experimental verification of this approach was given in several optical experiments, measuring the transmission/reflection of semiconductor heterostructures. In previous papers[35–38] we have demonstrated how the influence of many-body effects on the exciton line, e.g., carrier-induced line broadening, shift of the exciton resonance and band gap shrinkage show up in the phase and amplitude of transmitted/reflected light.

The semiconductor Bloch equation approach sketched above describes systems with a band structure in an electromagnetic field. In general, the two-particle problem in a surrounding medium needs a careful analysis of the Bethe-Salpeter equation for the two-particle Green's function.

A first approach in this direction was given in Refs. 3 and 4 using the dynamically screened ladder approximation. However, this result has some serious shortcomings, especially in the degenerate plasma. There, a static contribution in addition to the Hartree-Fock term, and, moreover, a division by the Pauli blocking factors $1-f_a(\mathbf{k}_1)-f_b(\mathbf{k}_2)$ occur. In a subsequent paper[27] it was shown that these shortcomings are produced by using an inappropriate retarded Green's function and by the treatment of the retardation of the screened potential by the Shindo approximation. The corrected effective Schrödinger equation was derived in Refs. 27 and 40 and for the EHP in Refs. 37 and 38. For an electron-hole pair system, both approaches are in full agreement for zero center-of-mass momentum.

Numerical solutions for the pair spectrum have been given in Refs. 35–38 using the SBE and in Refs. 3, 41, and 42 using the effective Schrödinger equation in the nondegenerate case.

Our numerical calculations were performed for zinc selenide (ZnSe) with an excitonic $1s$ ground state energy of 22.4 meV and effective electron and hole masses of $m_e = 0.15m_e^0$ and $m_h = 0.86m_e^0$, m_e^0 being the free electron mass. In Fig. 1 the imaginary part of the susceptibility χ is presented for a temperature of 30 K and different carrier densities. In order to present a better resolution of the different exciton states, we have used a logarithmic scale. The Mott transition is obviously generated by the decreasing band edge and takes place first for the higher exciton states. The position of the exciton nearly stays unchanged; there is only a weak shift to lower energies. The shift turns to higher energies if the temperature is decreased. This can be seen in

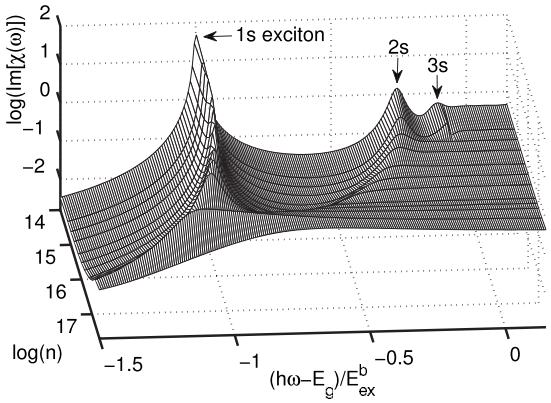

FIG. 1. Imaginary part of the susceptibility on a logarithmic scale for different carrier densities $n[\mathrm{cm}^{-3}]$ from the solution of the SBE (28). E_g is the band gap and E_{ex}^b is the $1s$-exciton energy.

Fig. 2, where the positions of the $1s$-exciton peak and of the band edge are shown for different temperatures.

The two-particle spectrum shown in Fig. 2 exhibits the following peculiarities: (i) There is a lowering of the band (continuum) edge due to the many-body effects contained in the self-energy. (ii) The exciton ground-state energy remains nearly constant up to higher densities. This follows from the approximative compensation of the many-particle effects for the bound states.[3] Moreover, at low temperatures, $\Theta(\mathbf{k},\mathbf{q},\omega)$ and, therefore, $\Sigma^r(\mathbf{k},\omega)$ are small, and Coulomb Hartree-Fock self-energy and Pauli blocking dominate. However, they nearly compensate each other at low densities, too, but lead to a weak shift for higher densities. (iii) The difference between band edge and exciton energy defines the effective ionization energy I^{eff}, which is lowered with increasing density. (iv) For $I^{\mathrm{eff}}=0$, the bound state vanishes and merges into the scattering continuum. This process is referred to as *Mott effect*, and the corresponding density is called Mott density.

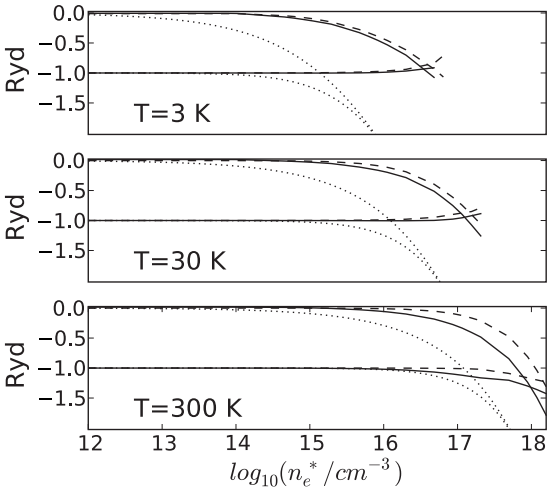

FIG. 2. Two-particle spectrum vs density in ZnSe: band edge (upper curves) and exciton ground state energy (lower curves). Solid lines: solution of the full SBE, dashed lines: solution with $\Theta(\mathbf{k},\mathbf{q},\omega)=0$ and $\Sigma^r(\mathbf{k},\omega)=0$ (Hartree-Fock approximation), dotted lines: static limit of $\Theta(\mathbf{k},\mathbf{q},\omega)$ and classical limit for $\Delta e^{sc}(\mathbf{k},\omega)$ (Debye approximation). Ryd denotes the excitonic Rydberg.

Above that point, the bound state does not exist, and the bound state energy is no longer a meaningful quantity. (v) Finally, the results for the exciton energy show a different behavior for high and low temperatures, i.e., we observe a blue (low T) or a red shift (high T), respectively.[35]

While the exciton energy appears in Fig. 2 as a well-defined line, in fact, the exciton is broadened due to a finite damping.[28] At low temperatures, however, this broadening is small: the excitonic full width at half maximum is $\gamma=0.012$ Ryd for 3 K and $\gamma=0.07$ Ryd for 30 K just below the Mott density, respectively.

In addition to our results from the solution of the full SBE (28), in Fig. 2 we show a comparison to two approximations: That is (i) a solution with screening effects being neglected in the SBE and only the HF energies and the Pauli blocking considered, i.e., $\Theta(\mathbf{k},\mathbf{q},\omega)=0$ and $\Sigma^r(\mathbf{k},\omega)=0$ (Hartree-Fock approximation). (ii) A further frequently used approximation is the static limit of $\Theta(\mathbf{k},\mathbf{q},\omega)$. It follows from Eq. (29) if $\bar{\omega}$ exceeds all other terms in the denominator. If furthermore, for $\Delta e^{sc}(\mathbf{k},\omega)$ [cf. Eq. (30)] the classical limit is applied, it leads to the Debye shift κe^2 (κ is the inverse screening length defined by $\kappa^2=(e^2/\epsilon_0\epsilon_r k_B T)(\frac{\partial n_e}{\partial \mu_e}+\frac{\partial n_h}{\partial \mu_h})$, ϵ_r is the background dielectric constant). Figure 2 shows that this approximation provides an inadequate description of both bound state energy and band edge even at room temperature. In particular, the Mott effect occurs at far too low densities. Static screening becomes a convenient approximation far above room temperature but completely fails at low temperatures.

V. CHEMICAL POTENTIAL AND DEGREE OF IONIZATION

The MAL given by Eq. (27) represents a relation between the chemical potentials of the EHP constituents (μ_e,μ_h,μ_X). While we assume μ_X to be the chemical potential of ideal bosons, Eq. (20), μ_e and μ_h [Eq. (21)] contain correlation contributions in the RPA quasiparticle energy $\epsilon_a(\mathbf{k})$, Eq. (10). The quasiparticle retarded self-energy of carriers is given in RPA by Eq. (31) or, in an alternative representation, by

$$\Sigma_a^{\mathrm{RPA}}(\mathbf{k},\omega)|_{\hbar\omega=\varepsilon_a(\mathbf{k})}=\Sigma_a^{\mathrm{HF}}(\mathbf{k})+\int\frac{d\mathbf{q}}{(2\pi)^3}\int\frac{d\omega'}{2\pi}\times\frac{[1-f^a(\varepsilon_a(\mathbf{q}))+n^B(\omega')]\hat{V}(\mathbf{k}-\mathbf{q},\omega')}{\varepsilon_a(\mathbf{k})-\varepsilon_a(\mathbf{q})-\hbar\omega'+i\Gamma_a(\mathbf{q})/2},\tag{34}$$

where $\hat{V}(\mathbf{q},\omega)$ is related to the correlation functions of the screened potential, Eq. (32) by $\hat{V}(\mathbf{q},\omega)=i[V^{>}(\mathbf{q},\omega)-V^{<}(\mathbf{q},\omega)]$. The quasiparticle energy $\varepsilon_a(\mathbf{k})$ is, in turn, given by Eq. (10).

In comparison to earlier calculations,[30] where quasiparticle energies $\varepsilon_a(\mathbf{k})$ on the right-hand side (r.h.s.) of Eq. (34) were replaced by kinetic energies and the damping $\Gamma_a(\mathbf{q})$ was neglected, we solve Eqs. (34) and (10) self-consistently by iteration. Our iteration procedure shows that both real and imaginary parts of the self-energy are reduced. These

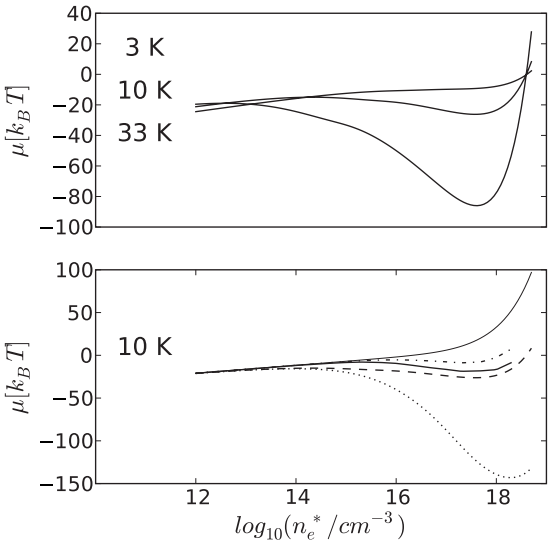

FIG. 3. Sum of the chemical potentials of electrons and holes $\mu=\mu_e+\mu_h$ vs density in ZnSe. Upper panel: μ^{RZR} for several temperatures T: 3 K (upper curve), 10 K (middle), 33 K (lower). Lower panel: μ^{iter} according to the self-consistent solution of Eqs. (34) and (10) (bold solid line), μ^{RZR} (dashed), μ^{id} (thin solid), μ^{HF} (dash-dotted), Debye approximation $\mu^{\mathrm{D}}=\mu_e^{\mathrm{id}}+\mu_h^{\mathrm{id}}-\kappa e^2$ (dotted), for $T=10$ K.

changes of the quasiparticle energies influence the chemical potentials, calculated from Eq. (21).

Figure 3 shows isotherms of the sum $\mu=\mu_e+\mu_h$ vs density. In order to illustrate the general behavior of the chemical potential, at first, we apply the idea of incomplete inversion of the density according to Eq. (22) with the correlation part given by the Padé formula from Ref. 30 and denote the resulting chemical potential by $\mu^{\mathrm{RZR}}=\mu_e^{\mathrm{id}}+\mu_h^{\mathrm{id}}+\Delta\mu_{eh}$.

The upper panel compares μ for several temperatures. At lower temperatures, a van der Waals loop occurs, i.e., a region with an instability $\partial\mu/\partial n\leq 0$, which may be a signal of a phase transition.[1,2,43] The lower panel shows a comparison of several approximations for μ: self-consistent iterative solution of Eqs. (34) and (10) (later on referred to as μ^{iter}), μ^{RZR}, Hartree-Fock and Debye approximations, and ideal chemical potential. What can be seen immediately is that the van der Waals loop is caused by many-particle effects. The latter ones are strongly overestimated by the Debye approximation. The other approximations deviate from the self-consistent result considerably, too. These quantitative differences will show up again in the ionization equilibrium, which is very sensitive to the actual form of the chemical potential.

Figure 4 represents a graphical solution of Eq. (27). For illustrative purposes we use again μ^{RZR} like in the upper panel of Fig. 3. Solid and dashed lines represent the r.h.s. and left-hand side (l.h.s.) terms of Eq. (27), respectively, for given temperatures T and total densities n_e. Their intersections indicate the possible values of the degree of ionization $\alpha(n_e,T)$. Here and in the following we consider only the ground state, i.e., $n=1$, $l=0$, $E_{nl}\equiv E_1$.

Isotherms of the degree of ionization as a function of the density obtained by numerical solution of the MAL (27) are

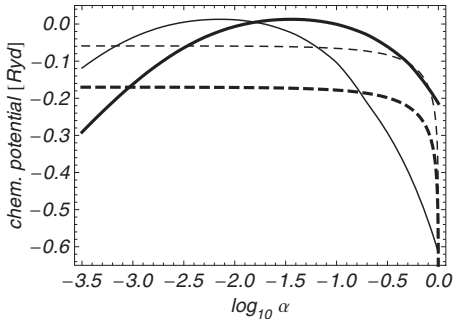

FIG. 4. Graphical solution of Eq. (27): chemical potential of the excitons μ_X [l.h.s. of Eq. (27); dashed lines] and sum of the chemical potentials of electrons and holes minus binding energy $\mu_e+\mu_h-E_1$ [r.h.s. of Eq. (27); solid lines] vs α for $T=20$ K and two densities: $n_e=10^{17}$ cm^{-3} (bold lines; single solution for α) and $n_e=5\times 10^{17}$ cm^{-3} (thin lines; three solutions for α).

shown in Fig. 5 (chemical potentials of carriers: μ^{iter}). We observe a very strong increase in α up to $\alpha=1$ at high densities due to the lowering of the ionization energy.[2,10] This behavior is usually referred to as *Mott transition* as a consequence of the Mott effect.

The comparison given in Fig. 6 shows the influence of the approximations applied for the chemical potential, cf. Fig. 3, on the degree of ionization. Obviously, the absolute position (and, as detailed investigations show, also the temperature dependence) of the Mott density vary for different approximations for the chemical potential.

At low enough temperatures, the curves exhibit a region where α is multivalued around the Mott density, i.e., a bistability occurs. The reason of this behavior is obvious from Figs. 3 and 4: the van der Waals loop in the chemical potential. Nevertheless, for lower densities there is only a single intersection of the curves, but for higher densities, three intersections are possible leading to three solutions for α for a given combination of temperature and density. Thus, we find a bistability (the intermediate solution is unstable), which may give rise to a first-order phase transition from an exciton gas to a fully ionized EHP (*Mott phase transition*). This effect has been addressed as a possible scenario for finding an excitonic condensate still at rather high densities (and, thus, at rather high temperatures).[44] It is, however, probably a theoretical artifact. Already the step from using μ^{RZR} to μ^{iter},

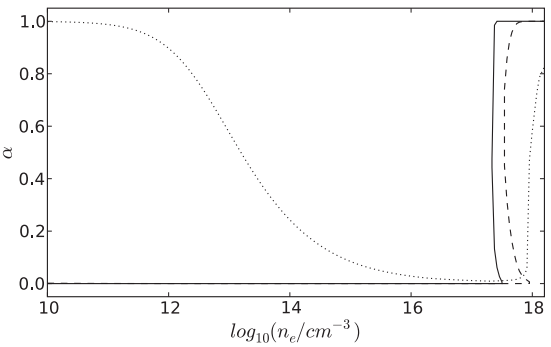

FIG. 5. Degree of ionization α vs density for several temperatures T, Eq. (27): 2 K (solid line), 10 K (dashed), and 30 K (dotted).

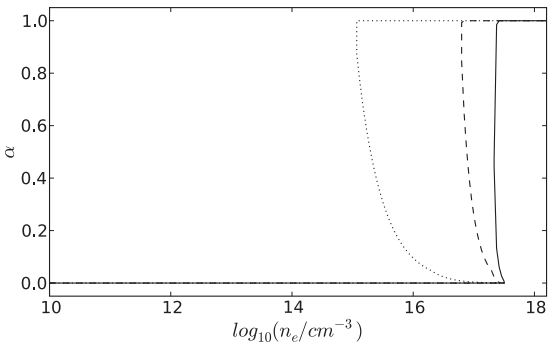

FIG. 6. Degree of ionization α vs density, Eq. (27), for $T=2$ K. Comparison of several approximations for the chemical potential: μ^{iter} (solid line), μ^{RZR} (dashed), and Debye approximation μ^{D} (dotted).

i.e., in particular, the inclusion of the single-particle damping and the complete inversion of the density instead of the incomplete one, reduces the density range of bistability significantly, cf. Fig. 6. The question whether the inclusion of the exciton-exciton interaction (which should be very important just below the Mott density since there are only excitons) would remove the bistability completely is still to be resolved. It is, however, very likely as similar experiences from the atom-atom interaction in the hydrogen plasma[21] show.

For an overview of the ionization state of the EHP, in Fig. 7, isolines $\alpha(n_e,T)$=const. in the density-temperature plane are shown. With increasing temperature at fixed density, thermal ionization takes place quite smoothly, while at fixed temperature with increasing density, the Mott transition appears as an abrupt jump from $\alpha=0$ to $\alpha=1$.

At lower temperatures we find a strong dominance of the excitons ($\alpha\approx 0$). Regarding them as noninteracting bosons, Bose-Einstein condensation (BEC) may be expected under the condition

$$(1-\alpha)n_e\Lambda_X^3 \geq 2.61. \tag{35}$$

This condition is given in Fig. 7 by the triangle bordered by the dashed line at the bottom. Note that the breakup of excitons at the Mott density does not mean a disappearance of the condensate. Instead, a closer investigation shows a smooth crossover to a BCS-type condensate at high densities.[18,19,45] Thus, the physical nature of the condensed particles changes, i.e., we find excitons below the Mott density, and Cooper-like electron-hole pairs far above it. To which extent the survival of the excitons as resonances just above the Mott density plays a role has still to be investigated.

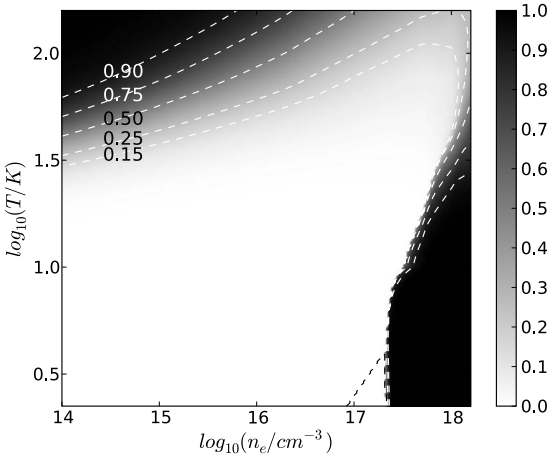

FIG. 7. Isolines of the degree of ionization in the density-temperature plane for ZnSe. The dashed triangle at the bottom borders the region where BEC of excitons is possible, cf. Eq. (35).

VI. SUMMARY AND OUTLOOK

The ionization equilibrium of an EHP has been investigated on a quantum statistical footing. Using the spectral function of carriers in extended quasiparticle approximation and transforming into a chemical picture, a very general mass-action law (MAL) has been considered which, in contrast to earlier papers, accounts for the Fermi/Bose character of carriers/excitons. This is indispensable for discussing the Mott transition at low temperatures and its interplay with a possible BEC of excitons. Many-body effects are included in the calculation of chemical potentials of carriers by their self-energies within quasiparticle approximation. The dynamical screened self-energies in RPA, depending itself on the chemical potentials again, have been computed self-consistently. In contrast to earlier papers not only the renormalization of the energy, but the damping (finite life time) of carriers have been incorporated, too. We have demonstrated that the changes of the chemical potentials due to many-body effects within our approach are strongly reduced in comparison to earlier approximations. In particular, an approximation based on static screening overestimates the influence of many-body effects at low temperatures by orders of magnitude (see Fig. 3).

The influence of many-body effects on the exciton energies has been obtained by using the semiconductor Bloch equations (SBE) considering the quasiparticle self-energies of carriers. We found that the Mott transition of excitons is shifted to higher carrier densities as compared to earlier approximations. For lower temperatures, the effects of dynamical screening in the SBE widely cancel and a simple model including the Coulomb Hartree-Fock renormalization (HF carrier energies and Pauli blocking) is applicable. Again, the approximation with static screening fails completely at low temperatures and is only valid far above room temperature (see Fig. 2).

This behavior is reflected in the degree of ionization, calculated with the generalized MAL for ZnSe and compared to the different approximations, too (see Figs. 5 and 6). The Mott transition, expressed by an abrupt increase in the degree of ionization, is shifted to higher carrier densities. For a temperature of 10 K, the Mott density is increased by more than one order of magnitude in comparison to those following by static screening approximation. In particular, the multivaluedness occurring around the Mott density is strongly suppressed within our approach. We assume that it will very likely vanish completely after inclusion of the exciton-exciton interaction. This assumption is based on calculations for the ionization equilibrium in hydrogen.[21]

Given the drastic deviations in chemical potentials, Mott density and extension of the ionization hysteresis that result from the mentioned earlier approximations for the many-particle effects, our previous calculations for Cu_2O as presented in Ref. 11 are to be taken with a grain of salt. They will be re-assessed on the present theoretical level in a forthcoming publication.

Finally, we have presented an overview of the ionization state in ZnSe as a function of temperature and density of carriers (see Fig. 7). Due to the increase in the Mott density, the possible window for the occurrence of BEC of noninteracting excitons is extended to higher temperatures.

ACKNOWLEDGMENTS

We would like to thank T. Schmielau (Sheffield), Th. Bornath, and H. Stolz (Rostock) for many fruitful discussions. This work was supported by the Deutsche Forschungsgemeinschaft (Collaborative Research Center SFB 652).

[1] R. Zimmermann, *Many-Particle Theory of Highly Excited Semiconductors* (Teubner, Leipzig, 1988).
[2] W. Ebeling, W. D. Kraeft, and D. Kremp, *Theory of Bound States and Ionization Equilibrium in Plasmas and Solids* (Akademie-Verlag, Berlin, 1976).
[3] K. Kilimann, W. D. Kraeft, and D. Kremp, Phys. Lett. **61A**, 393 (1977); R. Zimmermann, K. Kilimann, W. D. Kraeft, D. Kremp, and G. Röpke, Phys. Status Solidi B **90**, 175 (1978).
[4] H. Haug and D. B. Tran Thoai, Phys. Status Solidi B **85**, 561 (1978).
[5] Q. Y. Peng, T. Schmielau, G. Manzke, and K. Henneberger, J. Cryst. Growth **214-215**, 810 (2000).
[6] T. Schmielau, G. Manzke, D. Tamme, and K. Henneberger, Phys. Status Solidi B **221**, 215 (2000).
[7] C. F. Klingshirn, *Semiconductor Optics*, 3rd ed. (Springer, Berlin, 1995).
[8] C. Klingshirn, R. Hauschild, J. Fallert, and H. Kalt, Phys. Rev. B **75**, 115203 (2007).
[9] D. Snoke, Solid State Commun. **146**, 73 (2008).
[10] W. D. Kraeft, K. Kilimann, and D. Kremp, Phys. Status Solidi B **72**, 461 (1975).
[11] F. Richter, D. Semkat, D. Kremp, and K. Henneberger, Phys. Status Solidi C **6**, 532 (2009).
[12] L. V. Keldysh, in *Bose-Einstein Condensation*, edited by A. Griffin, D. W. Snoke, and S. Stringari (Cambridge University Press, Cambridge, 1995).
[13] S. A. Moskalenko, Fiz. Tverd. Tela (Leningrad) **4**, 276 (1962).
[14] E. Hanamura and H. Haug, Phys. Rep. **33**, 209 (1977).
[15] L. V. Keldysh and Yu. V. Kopaev, Sov. Phys. Solid State **6**, 2219 (1965).
[16] S. A. Moskalenko and D. W. Snoke, *Bose-Einstein Condensation of Excitons and Biexcitons and Coherent Nonlinear Optics with Excitons* (Cambridge University Press, Cambridge, 2000).
[17] J. Kasprzak *et al.*, Nature (London) **443**, 409 (2006).
[18] F. X. Bronold and H. Fehske, Phys. Rev. B **74**, 165107 (2006).
[19] D. Kremp, D. Semkat, and K. Henneberger, Phys. Rev. B **78**, 125315 (2008); D. Semkat, D. Kremp, and K. Henneberger, Phys. Status Solidi C **6**, 546 (2009).
[20] R. Redmer, Phys. Rep. **282**, 35 (1997).
[21] D. Kremp, M. Schlanges, and W.-D. Kraeft, *Quantum Statistics of Nonideal Plasmas* (Springer, Berlin, 2005).
[22] L. P. Kadanoff and G. Baym, *Quantum Statistical Mechanics* (Benjamin, New York, 1962).
[23] R. Zimmermann and H. Stolz, Phys. Status Solidi B **131**, 151 (1985).
[24] D. Kremp, W. D. Kraeft, and A. J. D. Lambert, Physica A **127**, 72 (1984).
[25] D. Kremp, W. D. Kraeft, and M. Schlanges, Contrib. Plasma Phys. **33**, 567 (1993).
[26] D. Kremp, M. K. Kilimann, W. D. Kraeft, H. Stolz, and R. Zimmermann, Physica A **127**, 646 (1984).
[27] Th. Bornath, D. Kremp, and M. Schlanges, Phys. Rev. E **60**, 6382 (1999).
[28] C. Klingshirn, Phys. Status Solidi B **244**, 3027 (2007).
[29] W. Stolzmann and W.-D. Kraeft, Ann. Phys. (Leipzig) **491**, 388 (1979).
[30] M. Rösler, R. Zimmermann, and W. Richert, Phys. Status Solidi B **121**, 609 (1984).
[31] W. Ebeling and W. Richert, Phys. Lett. **108A**, 80 (1985).
[32] G. W. Fehrenbach, W. Schäfer, J. Treusch, and R. G. Ulbrich, Phys. Rev. Lett. **49**, 1281 (1982).
[33] H. Haug and S. W. Koch, *Quantum Theory of the Optical and Electronic Properties of Semiconductors*, 4th ed. (World Scientific, Singapore, 1993).
[34] A. Girndt, F. Jahnke, A. Knorr, S. W. Koch, and W. W. Chow, Phys. Status Solidi B **202**, 725 (1997).
[35] G. Manzke, Q. Y. Peng, K. Henneberger, U. Neukirch, K. Hauke, K. Wundke, J. Gutowski, and D. Hommel, Phys. Rev. Lett. **80**, 4943 (1998).
[36] J. S. Nägerl, B. Stabenau, G. Böhne, S. Dreher, R. G. Ulbrich, G. Manzke, and K. Henneberger, Phys. Rev. B **63**, 235202 (2001).
[37] G. Manzke and K. Henneberger, Phys. Status Solidi B **234**, 233 (2002).
[38] M. Seemann, F. Kieseling, H. Stolz, R. Franz, G. Manzke, K. Henneberger, T. Passow, and D. Hommel, Phys. Rev. B **72**, 075204 (2005).
[39] G. Röpke and R. Der, Phys. Status Solidi B **92**, 501 (1979).
[40] T. Schmielau, Ph.D. thesis, Universität Rostock, 2001.
[41] S. Arndt, W. D. Kraeft, and J. Seidel, Phys. Status Solidi B **194**, 601 (1996).
[42] J. Seidel, S. Arndt, and W. D. Kraeft, Phys. Rev. E **52**, 5387 (1995).
[43] W. Ebeling, W. D. Kraeft, D. Kremp, and K. Kilimann, Phys. Status Solidi B **78**, 241 (1976).
[44] D. W. Snoke and J. D. Crawford, Phys. Rev. E **52**, 5796 (1995).
[45] P. Nozières and S. Schmitt-Rink, J. Low Temp. Phys. **59**, 195 (1985).